JOURNAL OF VIROLOGY, June 2004, p. 6449–6458 Vol. 78, No. 12
0022-538X/04/$08.00+0 DOI: 10.1128/JVI.78.12.6449–6458.2004

MCP-1 and CCR2 Contribute to Non-Lymphocyte-Mediated Brain Disease Induced by Fr98 Polytropic Retrovirus Infection in Mice: Role for Astrocytes in Retroviral Neuropathogenesis

Karin E. Peterson,[1] John S. Errett,[1] Tao Wei,[2] Derek E. Dimcheff,[1] Richard Ransohoff,[2] William A. Kuziel,[3] Leonard Evans,[1] and Bruce Chesebro[1]*

Laboratory of Persistent Viral Diseases, Rocky Mountain Laboratories, National Institute of Allergy and Infectious Diseases, National Institutes of Health, Hamilton, Montana 59840[1]; Department of Neurosciences, Lerner Research Institute, Cleveland Clinic Foundation, Cleveland, Ohio 44195[2]; and Autoimmune and Inflammatory Diseases, Protein Design Laboratories, Inc., Fremont, California 94555[3]

Received 15 October 2003/Accepted 16 February 2004

Virus infection of the central nervous system (CNS) often results in chemokine upregulation. Although often associated with lymphocyte recruitment, increased chemokine expression is also associated with non-lymphocyte-mediated CNS disease. In these instances, the effect of chemokine upregulation on neurological disease is unclear. In vitro, several chemokines including monocyte chemotactic protein 1 (MCP-1) protect neurons from apoptosis. Therefore, in vivo, chemokine upregulation may be a protective host response to CNS damage. Alternatively, chemokines may contribute to pathogenesis by stimulating intrinsic brain cells or recruiting macrophages to the brain. To investigate these possibilities, we studied a neurovirulent retrovirus, Fr98, that induces severe non-lymphocyte-mediated neurological disease and causes the upregulation of several chemokines that bind to chemokine receptors CCR2 and CCR5. Knockout mice deficient in CCR2 had reduced susceptibility to Fr98 pathogenesis, with significantly fewer mice developing clinical disease than did wild-type controls. In contrast, no reduction in Fr98-induced disease was observed in CCR5 knockout mice. Thus, signaling through CCR2, but not CCR5, plays an important role in Fr98-mediated pathogenesis. Three ligands for CCR2 (MCP-1, MCP-3, and MCP-5) were upregulated during Fr98 infection of the brain. Antibody-blocking experiments demonstrated that MCP-1 was important for retrovirus-induced neurological disease. In situ hybridization analysis revealed that MCP-1 was expressed by glial fibrillary acidic protein-positive astrocytes. Thus, astrocytes, previously not thought to play an effector role in the disease process were found to contribute to pathogenesis through the production of MCP-1. This study also demonstrates that chemokines can mediate pathogenesis in the CNS in the absence of lymphocytic infiltrate and gives credence to the hypothesis that chemokine upregulation is a mechanism by which retroviruses such as human immunodeficiency virus induce neurological damage.

Increased expression of chemokines is a common response to brain injury or disease and has been associated with human neurological diseases (16, 23, 39, 40). One effect of this chemokine response is the recruitment of antigen-specific T cells, which can cause neurological damage through direct damage to neurons or oligodendrocytes (23). However, increased chemokine expression is observed in neurological diseases, such as human immunodeficiency virus (HIV)-associated dementia (6, 16, 39) and Alzheimer's disease (40), where lymphocytic cell infiltration in the brain does not correlate with pathogenesis (17, 22). In these diseases, it is unclear whether chemokine upregulation is pathogenic or protective (7, 12, 15). Additionally, chemokine upregulation could simply be a response to pathogenesis rather than an active contributor or inhibitor of disease progression. It is difficult to distinguish cause versus effect in correlative observations of chemokine upregulation in human patients, in the absence of ways to block effector pathways in question. In contrast, using knockout mice, one can eliminate entire pathways by eliminating an individual ligand or its receptor. In the present study, we used knockout mice deficient in chemokine receptors CCR2 and CCR5 to analyze the role of certain chemokines in a non-lymphocyte-mediated neurological disease induced by the murine retrovirus, Fr98.

Infection of newborn mice with the murine polytropic retrovirus, Fr98, causes a neurological disease characterized by the development of severe ataxia, seizures, and ultimately death (26). In the brain, Fr98 infects endothelia and microglia and induces pathological changes that include the activation of astrocytes and microglial cells (26, 29). Previous analysis of mRNA expression in the brains of Fr98-infected mice revealed a substantial increase in the levels of monocyte chemotactic protein 1 (MCP-1), RANTES, macrophage inflammatory protein 1α (MIP-1α) and MIP-1β mRNA 3 to 4 days prior to the onset of clinical disease (25). In contrast, no upregulation of these genes was observed after infection with the avirulent retrovirus, Fr54. Thus, in this model, the upregulation of proinflammatory cytokines and chemokines correlates with the development of neurological disease rather with than retroviral infection per se. The increased expression of cytokine and chemokine genes does not appear to recruit lymphocytes to the

* Corresponding author. Mailing address: Rocky Mountain Laboratories, 903 S. 4th St., Hamilton, MT 59840. Phone: (406) 375-9354. Fax: (406) 363-9286. E-mail: bchesebro@niaid.nih.gov.

central nervous system (CNS) since no increase in CD3ε, CD4, CD8α, CD8β, or B220 mRNA expression (25) or increase in the number of CD3-positive cells (unpublished observations) is found in the CNS of Fr98-infected mice compared to mock-infected controls.

In the present study, we infected knockout mice deficient in either CCR2 or CCR5 with Fr98 to determine the contribution of these chemokine receptors to the development of retrovirus-induced neurological disease. Although several ligands for CCR5, including RANTES, MIP-1α, and MIP-1β, are upregulated in the brain after Fr98 infection, deletion of CCR5 had no effect on Fr98-induced neurological disease. In contrast, deletion of CCR2 resulted in a significant decrease in the incidence of disease after Fr98 infection. Kinetic analysis of the ligands for CCR2 demonstrated that MCP-1, MCP-3, and MCP-5 were upregulated in Fr98 infected mice starting at 12 days postinfection, with increased MCP-1 expression persisting through the late stages of clinical disease. In situ hybridization and immunohistochemistry revealed that different cell types were responsible for the expression of these ligands, with glial fibrillary acidic protein (GFAP)-expressing astrocytes producing MCP-1 and microglia or macrophage-like cells expressing MCP-5.

MATERIALS AND METHODS

Mice. Inbred Rocky Mountain White (IRW) mice were bred and housed at the Rocky Mountain Laboratories animal facility. CCR2$^{-/-}$ and CCR5$^{-/-}$ mice were generated on a mixed C57BL/6 × 129/Ola genetic background as described previously (14, 19, 20). The CCR2 and CCR5 knockout mutants were subsequently backcrossed to inbred BALB/c mice for six generations. Wild-type control BALB/c mice were obtained from Jackson Laboratories (Bar Harbor, Maine). All animal experiments were carried out in accordance with the regulations of the Rocky Mountain Laboratories Animal Care and Use Committee and the guidelines of the National Institutes of Health.

Viruses and intraperitoneal infection and antibody treatment of mice. The construction of virus clones Fr54 and Fr98 was described previously (26). Virus stocks were prepared from the supernatants of confluently infected *Mus dunni* fibroblast cells. Virus titers were determined by a focal infectivity assay using envelope-specific monoclonal antibody 514 (28). For intraperitoneal inoculation, IRW mice were injected with 10^4 focus-forming units (FFU) of virus within 24 h of birth. For antibody treatment, Fr98-infected IRW mice at 11 days postinfection were anesthetized using isoflurane and given 130 ng (8 μl) of polyclonal antibodies in 1% normal goat serum by intracerebral inoculation using a Hamilton syringe with a 30-gauge needle. The mice were observed daily for clinical signs of CNS disease, which was characterized by obvious signs of ataxia and/or seizures.

Virus inoculation using neural stem cells. The use of the neural stem cell line C17.2 as a vehicle for delivery of virus to the brain has been reported previously (21, 27, 35). C17.2 neural stem cells (NSC) were maintained in Dulbecco minimal essential medium with 1× sodium pyruvate and 10% fetal calf serum in Primaria tissue culture flasks. NSCs were infected by culturing 10^5 cells with 1× Polybrene and 10^5 FFU of Fr98 for 48 h and passaged until confluently infected. The cells were analyzed for virus infection by immunofluorescence using antibodies 514 or 720, which detect the Fr98 envelope protein (28). Prior to inoculation, Fr98 or mock-infected NSCs in nonconfluent flasks were harvested with trypsin-EDTA, washed twice in phosphate-buffered saline (PBS), and resuspended at 7.5×10^7 cells per ml in PBS with 0.1% trypan blue. Within 24 h of birth, mice were anesthetized by hypothermia and 4 μl of NSC suspension was injected into each ventricle using a Hamilton syringe with a 30-gauge needle for a final concentration of 6×10^5 NSC per mouse. Correct inoculation of cells into the ventricles was monitored by observing trypan blue staining in the ventricles. C17.2 neural stem cells were previously modified to produce β-galactosidase as a method of detection (34). Sagittal and coronal brain tissue sections from mock- and Fr98-NSC-inoculated wild-type and knockout mice showed the presence of NSC in multiple regions of the brain, including the olfactory bulbs, cortex, hippocampus, thalamus, and cerebellum, by immunohistochemistry for β-galalactosidase (27). Morphological analysis indicated that these cells did not undergo apoptosis (data not shown). Immunohistochemistry analysis of virus protein expression was performed on wild-type and CCR2 and CCR5 knockout mice to confirm the spread of virus from NSC to microglia as previously described (21, 27, 35). Mock-NSC- and Fr98-NSC-inoculated mice were monitored for clinical signs for 12 weeks postinoculation and were recorded as having disease when signs of severe ataxia and/or seizures were apparent. Inoculation of wild-type, CCR2$^{-/-}$, or CCR5$^{-/-}$ mice with mock-NSC did not induce signs of severe ataxia or seizures. Statistical analysis of disease development was done using Kaplan-Meier survival curve analysis.

RNase protection assay. Infected mice were exsanguinated by axillary incision under deep isoflurane anaesthesia. The brains were removed from infected mice at the indicated times, and the cerebrum and midbrain were separated from the cerebellum and brain stem. The tissues were immediately frozen in liquid nitrogen and stored at −80°C. Total RNA from the cerebrum or cerebellum was prepared using Trizol reagent (Life Technologies, Rockville, Md.) as specified by the manufacturer. For examination of mRNA from NSC, confluent cells were lysed using Trizol reagent and processed for RNA as specified by the manufacturer. RNA was quantified by spectroscopy at 260 nm, diluted to equal concentrations in hybridization buffer (BDPharmingen, San Diego, Calif.), and stored at −80°C until use. The RNA was then analyzed for specific cytokine and chemokine mRNA by using the RiboQuant System (BDPharmingen) as previously described (25).

Generation of probes for in situ hybridization. The template DNA for MCP-1 has been described previously (10). To generate template DNA for the MCP-3 and MCP-5 probes, we generated PCR products of cDNA from Fr98-infected mice, using forward primers CTGAAGCCAGCTCTCTCACTC for MCP-3 and CTTCGAAGTTGACCTCAA for MCP-5. The reverse primers were GGTTTC TGTTCAGGCACATTTC for MCP-3 and AATATCACACTGCCCGTGG for MCP-5. PCR products were inserted into the TOPO PCR2.1 vector (Invitrogen) and sequenced to confirm the correct sequence and orientation. Plasmids containing MCP-3 or MCP-5 in reverse orientation from the T7 promoter were digested with the restriction enzymes Sau3A1 for MCP-3 or XmaI for MCP-5. This created DNA templates of 237 bp for MCP-3 and 257 bp for MCP-5. Digoxigenin (DIG)-labeled antisense probes were generated using the DIG RNA labeling kit (Roche Molecular Biochemicals), T7 or T3 polymerase, and 0.5 to 1 μg of linearized template DNA as specified by the manufacturer's instructions. DIG-labeled probes were purified over RNAeasy columns (Qiagen, Valencia, Calif.). The probe concentration was calculated by using limiting serial dilutions of the probes on nylon membrane and comparing them to a known standard (Roche Molecular Biochemicals).

In situ hybridization. Brains from Fr98- or mock-infected mice were removed at 14 to 15 days postinfection, fixed in 4% paraformaldehyde for 3 to 5 days, dehydrated through a graded series of ethanol, and embedded in paraffin. Sections (4 μm thick) were cut using an RNase-free blade and placed on RNase-free SuperFrost slides (Fisher Scientific, Denver, Colo.). These sections were incubated overnight at 56°C and stored at room temperature until use. To remove paraffin, the sections were incubated overnight in xylene, rehydrated through a graded series of ethanol, and rinsed in 1× Tris-buffered saline (TBS; pH 7.5). Sections were incubated in 4% paraformaldehyde for 20 min at room temperature for fixation, rinsed in 1× TBS, incubated in 200 mM HCl for 15 min to denature the proteins, rinsed in 1× TBS, incubated for 10 min in 0.5% acetic anhydride in 0.1 M Tris (pH 8.0), and rinsed in TBS. Sections were incubated in 5 to 50 μg of proteinase K (Sigma, St. Louis, Mo.) per ml in 2 mM $CaCl_2$–1× TBS for 20 min at 37°C, rinsed in 1× TBS, and then incubated in 1× TBS at 4°C to stop the proteinase K digestion. The sections were then dehydrated through a graded series of ethanol, incubated in chloroform for 20 min, rehydrated through ethanol, and incubated in 2× SSC (1× SSC is 0.15 M NaCl plus 0.015 M sodium citrate) for 5 min. For prehybridization, 40 μl of hybridization solution (2× SSC, 10% dextran sulfate, 0.01% sheared salmon sperm DNA, 0.02% sodium dodecyl sulfate, 50% formamide) was added to each tissue section and the sections were incubated at 56°C for 1 h. For hybridization, DIG-labeled probes were diluted 1/50 to 1/200 in hybridization buffer and 20 μl of probe was added to each section. The sections were then coverslipped, heated to 95°C for 4 min, and hybridized overnight at 56°C. The coverslips were removed by incubating sections in 2× SSC for 15 min. Nonhybridized probe was digested with 20 μg of RNase A (Roche Molecular Biochemicals) per ml in 500 mM NaCl–10 mM Tris (pH 8.0) for 30 min at room temperature. Unbound probe was removed by rinsing sections in 2× SSC and then incubating them in 1× SSC–50% formamide for 1 h at 56°C. The sections were rinsed in 1× SSC, blocked in blocking buffer (1× blocking reagent in 1× maleic acid buffer [Roche Molecular Biochemicals]) for 30 min at room temperature, and incubated with alkaline phosphatase-labeled anti-DIG antibodies (Roche Molecular Biochemicals) at a 1/500 dilution in blocking buffer for 1 h at room temperature. To remove unbound anti-DIG

antibodies, the sections were rinsed twice in 1× TBS for 30 min. They were incubated in 0.1 M Tris (pH 8.2) for 15 min and then incubated with the substrate Fast-Red (Roche Molecular Biochemicals) for 12 to 72 h to detect chemokine-expressing cells. They were then either counterstained with hematoxylin or toluidine blue and coverslipped or used for immunohistochemistry.

Immunohistochemistry of in situ hybridization-labeled sections. Once color development was complete for in situ hybridization staining, sections were incubated for 1 h at 37°C in 1% normal goat serum (NGS) in PBS for detection of GFAP or in 1% normal rabbit serum (NRS) in PBS for detection of virus. The sections were then incubated with a 1/1,000 dilution of either rabbit anti-GFAP (Dako, Glostrup, Denmark) in 1% NGS or goat anti-murine retrovirus envelope protein (gp70) (28) in 1% NRS for 2 h at 37°C. They were rinsed in PBS and incubated with alkaline phosphatase-conjugated anti-rabbit or anti-goat antibodies (Jackson Immunoresearch, West Grove, Pa.) in 1% NGS or 1% NRS for 1 h at 37°C. They were then incubated with PBS for 20 min to remove unbound antibody and incubated with diaminobenzidine (DAB) substrate (Sigma-Ald rich) to detect positive cells. They were counterstained with hematoxylin or toluidine blue and coverslipped. In sections counterstained with toluidine blue, the DAB substrate appeared black, compared to the brown color associated with DAB staining in sections counterstained with hematoxylin.

Real-time PCR analysis of virus expression. Total RNA from the cerebrum or cerebellum and brain stem regions was isolated as described above for the RNase protection assay. The RNA was then treated with DNase (Ambion, Austin, Tex.) for 30 min to remove any contaminating DNA and purified over RNAeasy columns (Qiagen). Virus expression was analyzed by detection of the viral *gag* gene using the forward primer FB29 GAG-1169F (5′-AAACCAATGTGGCCA TGTCATT-3′), the reverse primer FB29 GAG-1244R (5′-AAATCTTCTAAC CGCTCTAACTTTCG-3′), and the probe FB29 GAG-1192T (5′-6FAM-ATCT GGCAGTCCGCCCCGG-TAMRA-3′) for analysis on an ABI PRISM 7900 sequence detection system (Applied Biosystems, Foster City, Calif.) Primer and probes from the Rodent GAPDH control reagent kit (Applied Biosystems) were used to detect glyceraldehyde 3-phosphate dehydrogenas (GAPDH) expression. Predeveloped primer and probe sets (Applied Biosystems) were used to detect MCP-1 and MCP-3 expression. MCP-2 expression was detected using the forward primer MCP2-252F (5′-CCAGACCAAGCAGGGTATGTC-3′), the reverse primer MCP2-315R (5′-CATGTACTCACTGACCCACTTCTGT-3′), and the probe MCP-2274T (5′-6FAM-CTCTGTGTAGACCCC-TAMRA-3′). MCP-5 expression was detected using the forward primer MCP5-21F (5′-ACA TGAAGATTTCCACACTTCTATGC-3′), the reverse primer MCP5-89R (5′-C AGCCAATACCTGAGGACTGATG-3′), and the probe MCP5-49T (5′-6FAM-CCTGCTCATAGCTACCA-TAMRA-3′). Reactions were run in triplicate using One-Step reverse transcription-PCR master mix (Applied Biosystems) in a 10-μl volume with approximately 10 ng of DNase-treated RNA, 500 nM each forward and reverse primer, and 250 nM probe. Lack of DNA contamination was confirmed by running the reactions without reverse transcriptase. The cycle number at which each sample reached a fixed fluorescence threshold (C_T) was used to quantitate gene expression. Data were calculated as the C_T value for virus *gag* expression minus the C_T value for GAPDH for each sample ($\Delta C_T = C_T gag\text{-}C_T$GAPDH) to determine the fold increase or decrease of *gag* expression relative to GAPDH expression in each sample. Standard-curve analysis of 10-fold serial dilutions of a positive control was used to analyze the efficiency of the PCR for each gene in order to correct for possible differences in the efficiencies of these separate PCRs.

RESULTS

Effect of chemokine receptor deletions on Fr98-induced neurological disease. Previously, the neurovirulent murine retrovirus Fr98 was shown to induce the mRNA expression of several chemokines including MCP-1, RANTES, MIP-1α, and MIP-1β in the CNS of infected mice 3 to 4 days prior to the onset of clinical disease (25). To analyze the role of the chemokines in Fr98-mediated pathogenesis, we used knockout mice deficient in either CCR2, the primary chemokine receptor for MCP-1, or CCR5, a chemokine receptor that binds RANTES, MIP-1α, and MIP-1β. Knockout mice are not available on the IRW background, the mouse strain primarily used for the study of polytropic retrovirus-induced disease (25, 26, 29). Therefore, we used BALB/c mice, which are not susceptible to Fr98-induced disease after intraperitoneal infection but do develop clinical disease after intraventricular inoculation with Fr98-NSC. The use of NSC as a method of virus infection has previously been shown to significantly increase the numbers of microglial cells infected by murine retroviruses (21, 27, 35). Brain tissue from BALB/c mice inoculated with Fr98-NSC had significantly higher levels of RANTES, MIP-1β, MIP-1α, and MCP-1 mRNA than did mock-infected controls (Fig. 1). This was not due to production of these chemokines by Fr98-NSC, since analysis of mock-infected and Fr98-NSC cultures demonstrated no detectable expression of cytokine or chemokine mRNA (data not shown). These results indicated that Fr98-NSC-infected BALB/c mice had a similar pattern of chemokine upregulation to that observed previously in IRW mice (25).

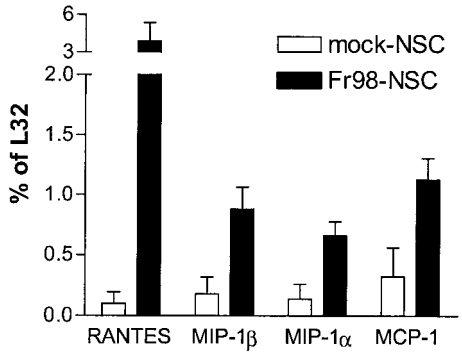

FIG. 1. Chemokine expression in Fr98-NSC- and mock-NSC-inoculated BALB/c mice. Total RNA from the brains of Fr98-NSC or mock-NSC mice at 21 days postinfection was analyzed for chemokine expression by using the RNase protection assay. Data are presented as the average of four mice per group and the standard error. Statistical analysis was done by a one-tailed Mann-Whitney test. *P* values were 0.014 for RANTES, 0.011 for MIP-1β, 0.029 for MIP-1α, and 0.029 for MCP-1.

Knockout BALB/c mice lacking expression of CCR5 or CCR2 were then studied to determine the effect of these chemokine receptors on Fr98-induced disease. Mice deficient in CCR5 inoculated with Fr98-NSC developed clinical signs of severe ataxia and seizures at the same rate and incidence as wild-type mice inoculated with Fr98-NSC (Fig. 2). Thus, despite the upregulation of RANTES, MIP-1α, and MIP-1β ligands for CCR5 during Fr98 infection, CCR5 was not required for Fr98-mediated neurological disease. In contrast, CCR2-deficient mice inoculated with Fr98-NSC had reduced incidence and delayed onset of severe ataxia and seizures compared to wild-type mice, indicating that CCR2 did contribute to disease pathogenesis (Fig. 2). The greatest difference in Fr98-NSC inoculated CCR2$^{-/-}$ mice compared to wild-type or CCR5$^{-/-}$ mice was during the initial 30 days postinoculation, with only 10% of CCR2$^{-/-}$ mice developing severe ataxia or seizures compared to 29 to 32% of CCR5$^{-/-}$ and wild-type mice. After 30 days postinfection, the rate of onset of clinical signs was similar in all three groups analyzed (Fig. 2). Thus, CCR2 appeared to contribute to the development of Fr98-mediated neurological disease, particularly in cases of early disease onset.

Effect of CCR2$^{-/-}$ on virus replication and spread. One possible effect of CCR2 deficiency on Fr98 infection could be

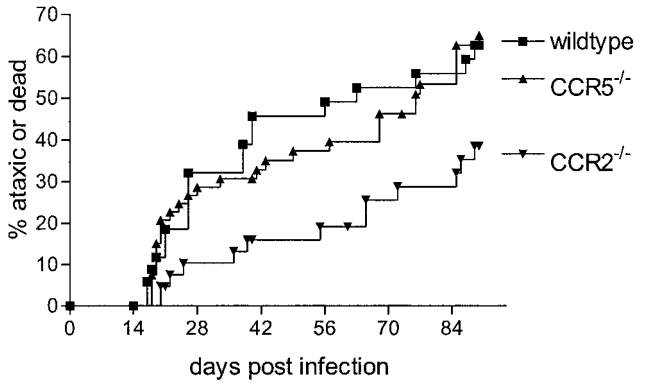

FIG. 2. Development of neurological disease in wild-type, CCR2$^{-/-}$, and CCR5$^{-/-}$ mice. Wild-type, CCR2$^{-/-}$, and CCR5$^{-/-}$ mice were inoculated with Fr98-infected NSC by intraventricular inoculation within 24 h after birth. The mice were then monitored for the development of clinical signs of severe ataxia, seizures, or death. Data are presented as the percentage of mice with severe ataxia or death for 35 wild-type mice, 57 CCR5$^{-/-}$ mice, and 46 CCR2$^{-/-}$ mice. Statistical analysis was done by Kaplan-Meier survival curve analysis using Graphpad Prism. The *P* value for the two-tailed log rank (Mantel-Haenszel) test for trends between all three groups was 0.022. The *P* values for the two-tailed log rank test between individual groups were 0.022 for CCR2$^{-/-}$ versus wild-type mice, 0.95 for CCR5$^{-/-}$ versus wild-type mice, and 0.011 for CCR2$^{-/-}$ versus CCR5$^{-/-}$ mice.

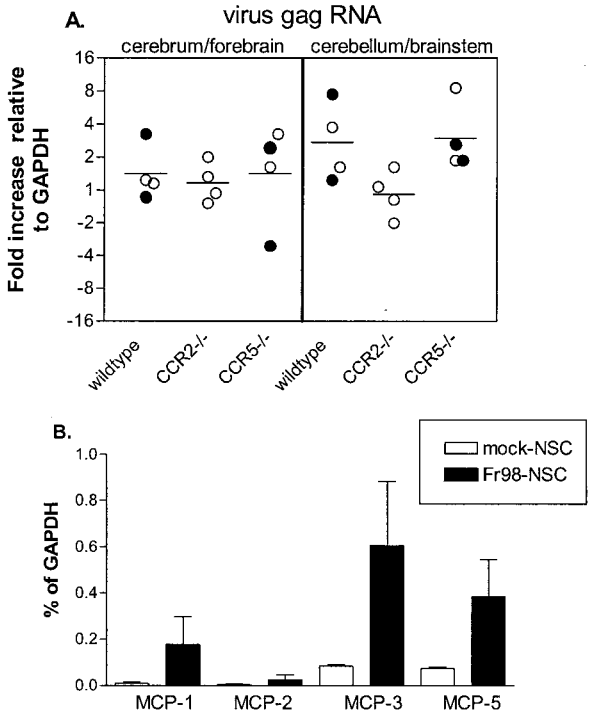

FIG. 3. (A) Virus *gag* mRNA expression in the cerebrum and cerebellum-brain stem of Fr98-NSC-inoculated wild-type, CCR2$^{-/-}$, and CCR5$^{-/-}$ mice. Virus *gag* mRNA expression was determined using real-time PCR. Data are shown as the difference of *gag* mRNA relative to GAPDH mRNA expression ($-\Delta C_T$). Each circle represents a single animal; open circles indicate mice with no clinical signs of ataxia, while solid circles indicate mice with clinical signs of ataxia. Statistical analysis was done using a two-tailed one-way analysis of variance with Newman-Keuls post hoc test. (B) MCP mRNA expression in mock-NSC- or Fr98-NSC-infected mice at 21 days postinfection as detected by real-time PCR. Data are presented as a percentage of GAPDH and are the average and standard error for three mice per group. Statistical analysis was done by a one-tailed Mann-Whitney test. *P* values were 0.05 for MCP-1, 0.35 for MCP-2, 0.05 for MCP-3, and 0.05 for MCP-5.

via restriction of virus replication and spread. To test this possibility, we analyzed virus infection in Fr98-NSC-inoculated CCR2$^{-/-}$, CCR5$^{-/-}$, or wild-type mice by real-time PCR at 3 to 4 weeks postinfection, the time of greatest difference in disease development in CCR2$^{-/-}$ mice compared to CCR5$^{-/-}$ or wild-type mice. No difference in viral *gag* gene expression was observed in the cerebrum or forebrain of CCR2$^{-/-}$ mice compared to that in wild-type or CCR5$^{-/-}$ mice (Fig. 3A). A slight but not statistically significant decrease in the level of viral *gag* mRNA was found in the cerebellum and brain stem region of CCR2$^{-/-}$ mice compared to wild-type or CCR5$^{-/-}$ mice. Additionally, no significant difference was observed in viral *gag* protein levels among the three groups (data not shown). By immunohistochemistry, the number and location of virus-infected microglial and endothelial cells in CCR2$^{-/-}$ mice was similar to those in wild-type controls (Fig. 4A and B). Thus, the CCR2 deficiency did not appear to have a significant effect on Fr98 replication or spread in the brain.

Expression of ligands for CCR2 during Fr98 infection. Since deletion of CCR2 did not affect virus levels in the brain, it is probable that the effect of CCR2 on Fr98-mediated neurological disease was due to chemokine binding and signaling through CCR2. CCR2 binds several chemokines, primarily MCP-1, MCP-2, MCP-3, and MCP-5 (3, 11, 30). We were therefore interested in determining if the expression of these genes was upregulated by Fr98 infection and if any of these genes were upregulated prior to disease onset. By real-time PCR analysis, an increase in the levels of MCP-1, MCP-3, and MCP-5 mRNA, but not MCP-2 mRNA, was detected in the brains of Fr98-NSC-inoculated BALB/c mice compared to age-matched controls inoculated with mock-infected NSC (Fig. 3B). Thus, this increase in the expression of several ligands for CCR2 correlated with Fr98-mediated neurological disease.

Since the onset of severe clinical signs ranged from 17 to 89 days in Fr98-infected BALB/c mice (Fig. 2), it would be difficult to study the kinetics of gene expression in relation to disease development. Therefore, we used IRW mice, where the onset of severe ataxia and seizures ranges only from 15 to 16 days postinfection and occurs in 100% of Fr98-infected mice (25). mRNA from the brains of mice infected with Fr98 or the avirulent virus, Fr54, was analyzed for expression of MCP-1, MCP-2, MCP-3, MCP-5, and CCR2 starting at 7 days postinfection until the onset of clinical signs in Fr98-infected mice on day 15.

Interestingly, the four ligands for CCR2 did not follow the same kinetic patterns of expression after Fr98 infection (Fig. 5). MCP-1 mRNA expression was increased in Fr98-infected IRW mice beginning at 12 days postinfection and remained elevated over the course of disease development (Fig. 5A), similar to previous observations (25). MCP-2 expression was not upregulated during Fr98 infection, with all samples below detection by real-time PCR (data not shown). Expression of both MCP-3 and MCP-5 was increased in Fr98-infected mice at 12 days postinfection, similar to MCP-1, but was downregu-

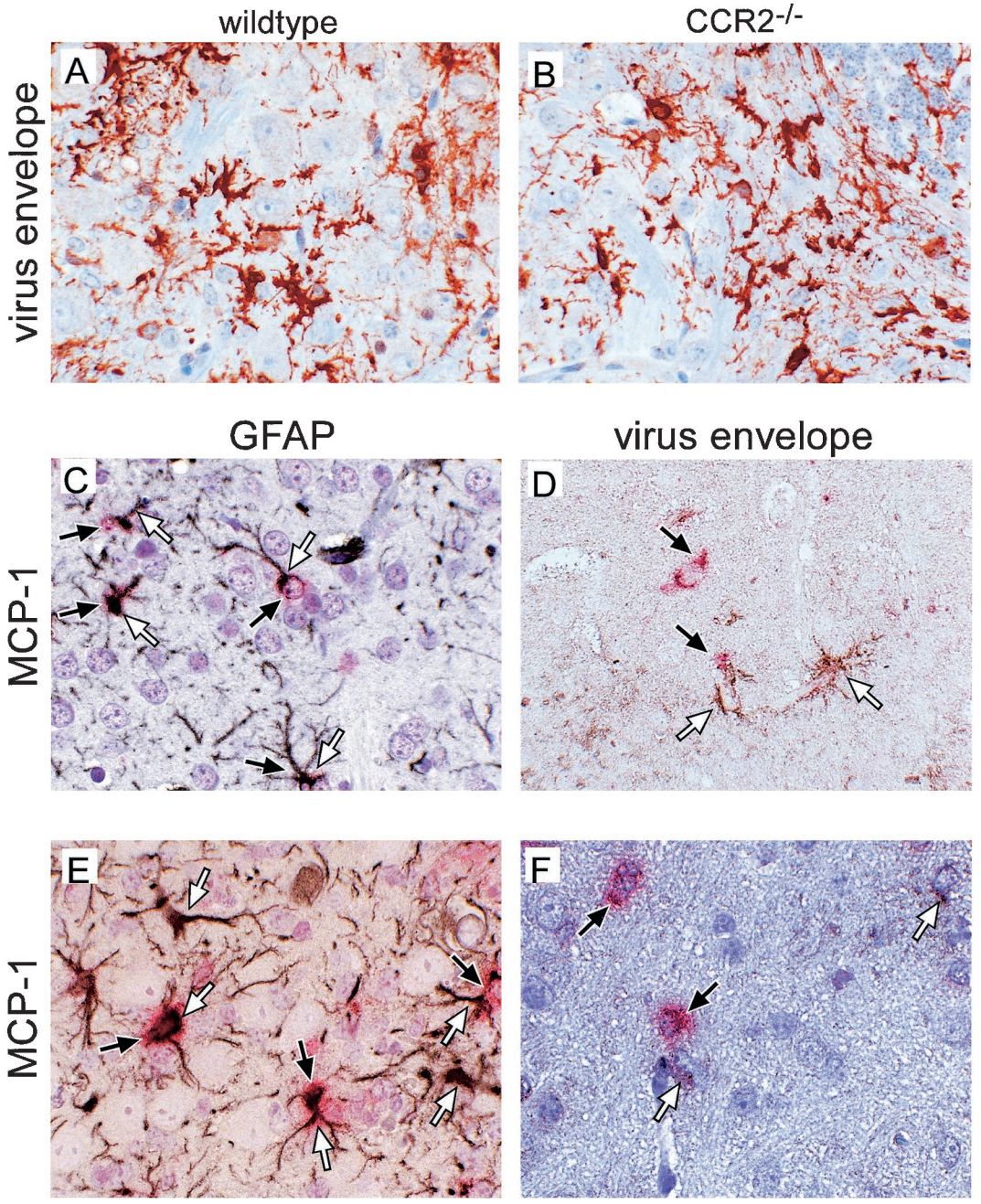

FIG. 4. (A and B) Immunohistochemistry analysis of viral envelope expression in the cerebellum in wild-type (A) or CCR2$^{-/-}$ (B) mice. Sections were incubated with an antiviral envelope antibody, followed by horseradish peroxidase-conjugated antigoat antibodies and developed with aminoethylcarbazole. All photographs were taken with a digital camera. (C to F) In situ hybridization and immunohistochemistry analysis of MCP-1 expression in Fr98-infected IRW mice (C and D) or Fr98-NSC-inoculated BALB/c mice (E and F). Sections were hybridized with DIG-labeled antisense RNA for MCP-1 and developed using Fast Red stain (red cytoplasm color, black arrows). No Fast Red-positive cells were observed in mock-infected mice for any of the above chemokines (data not shown). The sections were then incubated with anti-GFAP (C and E) or anti-gp70 virus envelope (D and F) and developed with DAB (brown/black positive color, white arrows). Sections were counterstained with hematoxylin (A, B, and D to F) or toluidine blue (C). Photographs were taken with a digital camera. Magnification, ×40.

lated by time of clinical signs (Fig. 5B and C). Thus, MCP-1, MCP-3, and MCP-5 were all upregulated at some stage during Fr98 infection and conceivably could contribute to disease pathogenesis.

In addition to CCR2 ligand expression, changes in CCR2 expression during disease development could have an impact on pathogenesis. Analysis of CCR2 mRNA expression revealed a slight increase in mRNA expression at 11 to 12 days postinfection in Fr98-infected mice compared to Fr54-infected mice (Fig. 5D). However, by the time of clinical-disease onset,

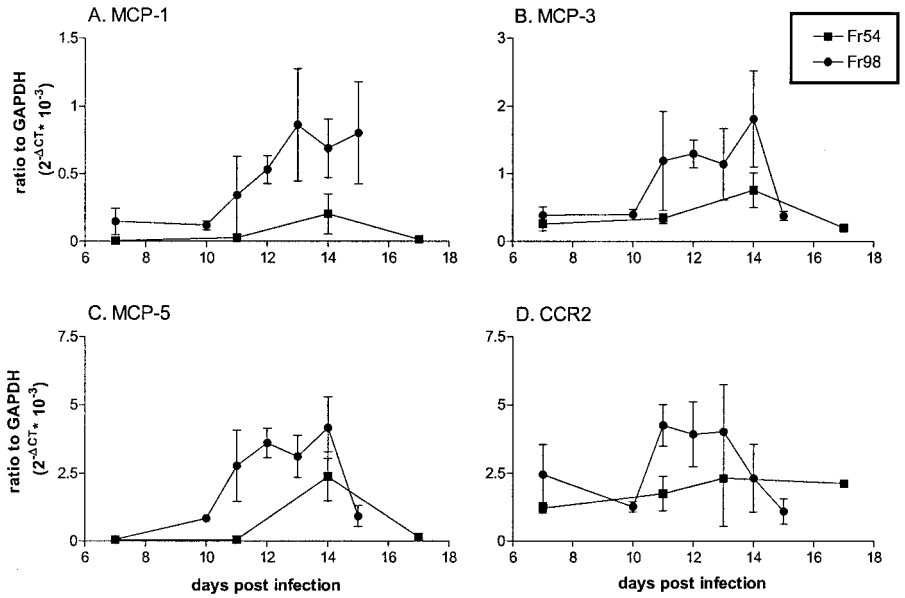

FIG. 5. Kinetic analysis of mRNA expression of MCP-1 (A), MCP-3 (B), MCP-5 (C), and CCR2 (D) in Fr54- or Fr98-infected IRW mice. mRNA expression was determined using real-time PCR. Data are shown as the average difference of the gene of interest relative to GAPDH mRNA expression on a linear scale ($2^{-\Delta CT}$). The data are presented as the average for two to four mice per time point for Fr54 and three to seven mice per time point for Fr98; error bars indicate standard error.

CCR2 levels had decreased to steady-state levels. Since activated but not resting microglial cells express CCR2, the upregulation of CCR2 during Fr98 infection may be due to the activation of these cells. Alternatively, it may indicate the recruitment of CCR2-positive cells to the brain.

Cell-specific expression of MCP-1, MCP-3, MCP-5, and CCR2. To gain a better understanding of how the MCP chemokines may be functioning in the brain, we wanted to determine the cell types and regions of the brain where these chemokines were expressed. To do this, we used in situ hybridization to analyze brain tissue from IRW mice at 13 and 15 days postinfection, the time points at which MCP-5, MCP-3, or MCP-1 were expressed at the highest level. Tissue sections of brains from mock and Fr98-infected mice were analyzed for the expression of MCP-1, MCP-3, and MCP-5 by using DIG-labeled antisense RNA probes. Between 7 and 20 MCP-1-positive cells per midsagittal brain section were detected in Fr98-infected mice (Fig. 4C and D, red stain), while no MCP-1-positive cells were detected in similar brain tissue from mock-infected mice (data not shown). Similar results were obtained using tritium-labeled antisense MCP-1 probes (data not shown). MCP-1-positive cells had astrocyte morphology and were located primarily in the internal capsule but were also detected in the thalamus, hippocampus, cortex, and cerebellum. Dual staining of MCP-1-positive cells with an astrocyte-specific marker, anti-GFAP, demonstrated that the MCP-1-positive cells were astrocytes (Fig. 4C). However, less than 1% of GFAP-positive cells had detectable MCP-1. Thus, a subset of astrocytes, through the production of MCP-1, may be active contributors to retroviral pathogenesis in the brain.

The production of MCP-1 by only a low percentage of astrocytes suggested that these cells were a subpopulation that may have been selectively stimulated. Astrocytes are not normally infected by Fr98. However, to rule out the possibility that the MCP-1-producing astrocytes were a subpopulation of infected astrocytes, we dually stained tissue sections for MCP-1 mRNA and virus protein expression. MCP-1-positive cells were not positive for virus protein (Fig. 4D), indicating that these cells were not productively infected with virus. Several MCP-1-positive cells were located near but not adjacent to virus-positive cells (Fig. 4D and data not shown) suggesting that infected microglial cells may stimulate astrocytes to produce MCP-1.

To study cell-specific expression of MCP-3, MCP-5, and CCR2, we analyzed IRW mice at both 13 and 15 days postinfection, since peak mRNA expression of these genes occurred at 12 to 14 days postinfection (Fig. 5). No MCP-3-positive cells were detectable in Fr98-infected IRW mice at 13 or 15 days postinfection by in situ hybridization, despite the upregulation of MCP-3 mRNA. Possibly, MCP-3 is produced at a low level by numerous cells and is thus present below the limit of detection by in situ hybridization. Similar to the finding with MCP-3, no positive CCR2 cells were detectable by in situ hybridization (data not shown). Since CCR2 mRNA is detectable in both IRW and BALB/c mice, it is possible that expression levels of CCR2 are too low in individual cells for detection of mRNA by in situ hybridization.

In contrast to MCP-3, numerous MCP-5-positive cells were detected, with about 40 to over 100 positive cells per midsagittal brain section, located primarily in the cortex (Fig. 6A and C) and cerebellum (Fig. 6B and D) of Fr98-infected mice at 13 days postinfection, No positive cells were detected in mock-infected controls. Dual staining with antibodies specific for GFAP (Fig. 6A to C) or gp70 (Fig. 6D) revealed that MCP-5-positive cells were not astrocytes or infected microglial cells. Surprisingly, about 50% of the positive cells were located in or

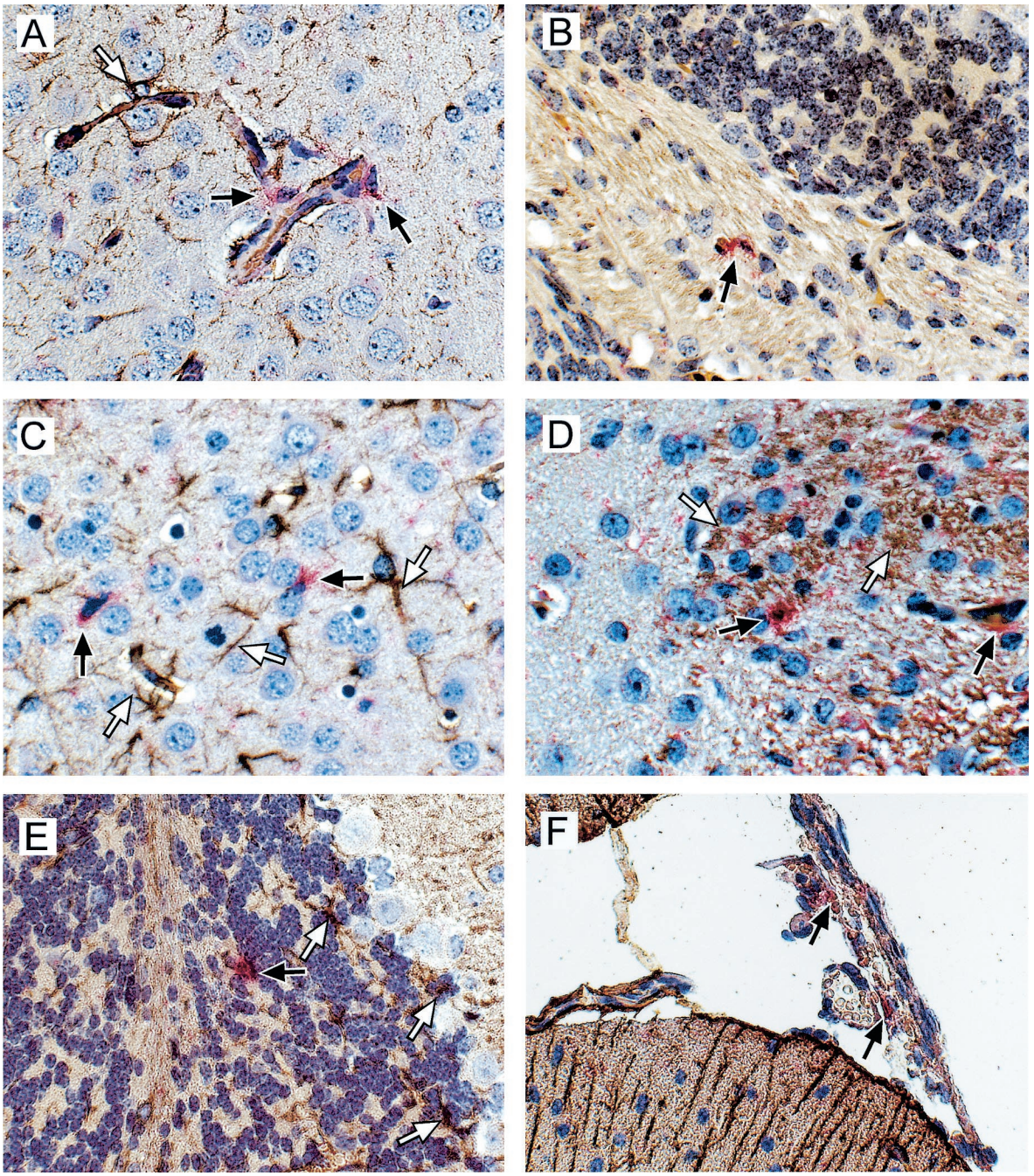

FIG. 6. In situ hybridization and immunohistochemistry analysis of MCP-5 expression in Fr98-infected IRW mice (A to D) or Fr98-NSC-inoculated BALB/c mice (E and F). Sections were hybridized with DIG-labeled antisense RNA for MCP-5 and developed using Fast Red stain (red cytoplasm color, black arrows). No Fast Red-positive cells were observed in mock-infected mice for any of the above chemokines (data not shown). Sections were then incubated with anti-GFAP (A, C, E, and F), no antibody (B), or anti-gp70 virus envelope (D) and developed with DAB (brown/black positive color, white arrows). All sections were counterstained with hematoxylin. Photographs were taken using a digital camera. Magnification, ×40.

around blood vessels (Fig. 6A), suggesting that many of the MCP-5-positive cells could be infiltrating macrophages. The other portion of MCP-5-positive cells was scattered throughout the cortex (Fig. 6C) or localized in the white matter tracts of the cerebellum (Fig. 6B and D). Nuclear morphology suggested that these cells were either brain macrophages or microglial cells, but due to technical difficulties with the dual staining of these tissues, we were not able to confirm the identity these cell types by antibody staining. Analysis of Fr98-infected mice at 15 days postinfection revealed considerably fewer MCP-5-positive cells, consistent with the decrease in MCP-5 mRNA expression at the time of disease (Fig. 5).

Additionally, these cells were not located next to blood vessels but were located in the parenchyma of the cerebral cortex and in the white matter tracts of the cerebellum. Thus, the MCP-5-expressing cells from day 13 postinfection appear to have either lost MCP-5 expression or migrated out of the brain prior to the onset of neurological disease in Fr98-infected IRW mice.

Expression of MCP-1 MCP-3, and MCP-5 in BALB/c mice. To determine if the cellular sources of the chemokines were similar in IRW and BALB/c mice, we analyzed the expression of MCP-1, MCP-3, and MCP-5 in BALB/c mice with clinical signs of neurological disease. Similar to the findings in the IRW mice, MCP-1-positive cells in BALB/c mice inoculated with Fr98-NSC were positive for GFAP (Fig. 4E) and not for virus (Fig. 4F) at the time of clinical disease. No MCP-1-positive cells were detected in mock-infected NSC-inoculated BALB/c mice.

Similar to IRW mice, no cells positive for MCP-3 were detected in the Fr98-NSC-inoculated BALB/c mice with clinical disease (data not shown). Analysis for MCP-5 expression in Fr98-NSC-inoculated BALB/c mice revealed a few MCP-5-positive cells scattered in the cerebellum (Fig. 6D) and several MCP-5-positive cells in the meninges of the brain (Fig. 6F). Dual staining with GFAP and virus envelope antibodies demonstrated that these cells were not astrocytes (Fig. 6D and F) or infected with virus (data not shown). The meningeal location of MCP-5-positive cells during the onset of neurological disease in BALB/c mice was not observed in IRW mice, although the type of cell producing MCP-5 may be the same.

Treatment of mice with antibodies against MCP-1, MCP-3, and MCP-5. The expression of MCP-1 and MCP-5 by different cell types (Fig. 4 and 6) and the different kinetics of expression (Fig. 5) suggested that these chemokines may not contribute equally to disease. To determine whether the three upregulated ligands for CCR2 contributed to neurological disease, we treated Fr98-infected IRW mice with anti-MCP-1, anti-MCP-3, or anti-MCP-5 polyclonal antibodies by direct intracranial inoculation at 11 days postinfection, the initial time point of increased chemokine expression (Fig. 5). No effect on clinical disease was observed in mice treated with anti-MCP-3 or anti-MCP-5 antibodies compared to immunoglobulin (Ig)-treated controls (Fig 7). However, mice that received a single injection of anti-MCP-1 had significantly delayed onset of clinical disease compared to Ig-treated controls (Fig. 7). Thus, MCP-1, but not MCP-3 or MCP-5, contributes to Fr98-induced pathogenesis.

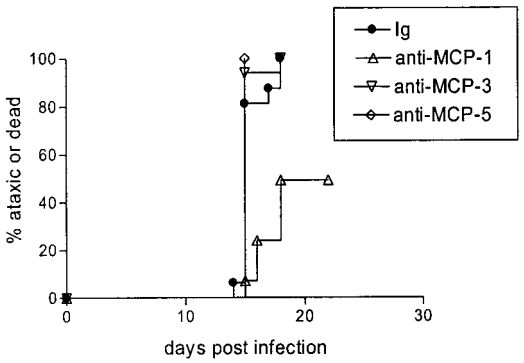

FIG. 7. Effect of anti-MCP-1, anti-MCP-3, or anti-MCP-5 on neurological disease development following Fr98 infection. IRW mice were infected with 10^4 FFU of Fr98 by intraperitoneal inoculation within 24 h after birth. At 11 days postinfection, the mice were treated with 130 ng of antibody in 1% NGS–PBS by intracranial inoculation. They were then monitored for signs of ataxia and seizures. Data are presented as the percentage of mice with severe ataxia or dead for 12 to 16 mice per group. Statistical analysis was done by Kaplan-Meier survival curve analysis using Graphpad Prism. The *P* value for the two-tailed log rank test for trend between all three groups was 0.015. The *P* values for the two-tailed log rank test between individual groups were 0.006 for control Ig versus anti-MCP-1-treated mice, 0.76 for control Ig versus anti-MCP-3-treated mice, and 0.35 for control Ig versus anti-MCP-5-treated mice.

DISCUSSION

In previous studies of Fr98 neurovirulence, development of neurological disease correlated with increased expression of several chemokines including MCP-1, RANTES, MIP-1α, and MIP-1β (25). Many of these chemokines are also associated with neurological disease induced by other retroviruses including HIV and simian immunodeficiency virus (6, 12, 16, 41). However, it was unclear if the upregulation of these chemokines was produced as a response to protect neurons, as has been suggested by some in vitro studies (7, 15), or if the chemokines were responsible for mediating neuropathogenesis. To analyze the role of these chemokines in Fr98-mediated neurovirulence in vivo, we inoculated mice deficient in the chemokine receptors CCR2 or CCR5 with Fr98-infected NSC. Interestingly, $CCR2^{-/-}$ mice were less susceptible to Fr98-induced neurological disease than were wild-type or $CCR5^{-/-}$ mice (Fig. 2), demonstrating that signaling through CCR2 plays a pathogenic role in this model. The ability of anti-MCP-1 antibodies, but not anti-MCP-3 or anti-MCP-5 antibodies, to delay disease development indicates that MCP-1/CCR2 interactions are critical for induction of neurological disease. Since MCP-1 is produced by astrocytes, this demonstrates for the first time an important role for uninfected astrocytes in retrovirus-induced neurological disease.

One possible mechanism by which MCP-1/CCR2 may contribute to neuropathogenesis is through the recruitment of peripheral macrophages. Studies with transgenic mice expressing MCP-1 under the GFAP promoter demonstrated that MCP-1 can recruit macrophages to the brain (8). However, since these MCP-1 transgenic mice did not develop any signs of clinical disease (8), macrophage infiltration alone does not cause neurological disease. In the Fr98 model of neurovirulence, we have been unable to detect significant macrophage infiltration in the brain at the time of clinical disease (unpublished data). This does not preclude the possibility that a small number of macrophages, below the limits of detection by immunohistochemistry or flow cytometery, contribute to pathogenesis. Additionally, peripheral macrophages may invade and damage the brain but may leave prior to the onset of clinical disease, similar to the abundance and scarcity of MCP-5-positive cells prior to and at the onset of clinical disease (Fig. 6).

Another mechanism by which MCP-1/CCR2 may contribute to neuropathogenesis is through the stimulation and/or activation of intrinsic brain cells. CCR2 protein expression has been found in the CNS on astrocytes, neurons (1), and activated

microglia (9). Addition of MCP-1 to in vitro cultures protects both neurons and astrocytes from *N*-methyl-D-aspartate-induced apoptosis, suggesting that CCR2 stimulation may have a protective effect on these cell types. However, direct injection of MCP-1 in the brain induced lethargy in rats (1), indicating that MCP-1 could have negative effects on neuronal function. It is possible that the effect of MCP-1 on astrocytes or neurons depends on the activation state of the cell. Thus, the other cytokines or chemokines upregulated during retrovirus infection may influence whether MCP-1 is harmful or protective to neurons or astrocytes.

In other studies, increased pathogen loads and in some cases increased mortality was found in CCR2$^{-/-}$ mice after infection with viruses such as mouse hepatitis virus (5) or bacteria such as *Mycobacterium tuberculosis* (24) or *Listeria monocytogenes* (18). However, in these studies, the primary role of CCR2 appeared to be the recruitment of the antigen-specific T cells to the site of infection rather than a direct effect on pathogen growth or immune cell activation. In Fr98 infection, no recruitment of lymphocytes is observed (25). This lack of T-cell infiltration may explain why CCR2 does not appear to be necessary for host defense against Fr98 infection, since neither disease induction (Fig. 2) nor virus levels (Fig. 3) were increased in Fr98-infected NSC-inoculated CCR2$^{-/-}$ mice compared to wild-type controls.

It remains unclear why Fr98 infection does not result in lymphocyte infiltration of the brain, since several proinflammatory cytokines and chemokines are upregulated during infection (Fig. 1) (25). Similar findings were observed with Sindbis virus and Borna disease virus infections of neonatal rats, with the induction of cytokine and/or chemokine expression and the development of severe neurological disease in the absence of significant lymphocytic infiltration (4, 32, 36). It is possible that the immature lymphocytes in neonatal animals cannot be activated sufficiently and become tolerant to the virus, as suggested by various models of neonatal tolerance (31). Alternatively, adhesins and other molecules necessary for the attachment and entry of lymphocytes into the brain may not be expressed at sufficient levels in neonatal brain capillaries. In the absence of lymphocyte activation and/or recruitment, the production of chemokines such as MCP-1 by the innate immune response appears to be detrimental rather than protective, as indicated by the present study.

The present results may have interesting implications for the development of HIV dementia, for which correlative studies have suggested a role for MCP-1 in brain pathogenesis. For example, increased MCP-1 levels in the cerebrospinal fluid correlate with development of neurological disease in HIV-infected patients (16), and the HIV tat protein induces MCP-1 production by astrocytes in vitro (6). Additionally, an allele of the MCP-1 gene that is associated with higher levels of MCP-1 in tissue correlated with increased risk of dementia in HIV-infected patients (12). However, it is not clear whether the increased expression of MCP-1 in HIV-associated dementia directly contributes to neuropathogenesis or is merely a host response to disease development. In patients with HIV infection, several types of pathology have been observed, including neuronal cell apoptosis, astrocytosis, microglial nodules, and microglial giant cell formation (2, 17). Similarly astrocytosis and microglial nodules are the primary pathology associated with Fr98 infection in mice (26). Furthermore, both Fr98 and HIV infect primarily microglia in the brain (17, 26). It is possible that these two viruses may induce neurological disease by analogous mechanisms. Our present results with Fr98 retroviral infection implicate the upregulation of the MCP chemokines and signaling through CCR2 as an important mediator of neuropathogenesis. Thus, similar to Fr98, MCP-1 signaling through CCR2 may be an important component of HIV-induced neuropathogensis.

Three ligands for CCR5, including MIP-1α, MIP-1β, and RANTES (33, 37), are all upregulated in HIV patients with dementia compared to patients without dementia, suggesting that chemokine signaling through CCR5 could affect neuropathogenesis. However, CCR5 is directly involved as a coreceptor for HIV infection of microglial cells (13), and it is difficult to separate out this effect on viral replication from possible additional roles of CCR5 in HIV neuropathogenesis. In the Fr98 model of neurological disease, the upregulation of MIP-1α, MIP-1β, and RANTES is also associated with the development of neurological disease. Unlike HIV, Fr98 does not use CCR5 as a coreceptor for entry into microglial cells. In the present study, deletion of the CCR5 gene had no effect on Fr98-mediated neurological disease (Fig. 2). Thus, MIP-1α, MIP-1β, and RANTES, although upregulated, surprisingly did not appear to contribute to disease pathogenesis via CCR5 signaling. However, since RANTES and MIP-1α also bind to CCR1 (38) and since CCR1 is present in Fr98-infected mice (25), these chemokines may play a role in disease pathogenesis by signaling through CCR1 instead of CCR5. At present, CCR1-deficient mice are available only on the C57BL mouse background, which blocks susceptibility to Fr98-induced neurological disease. Therefore, the study of CCR1-deficient mice requires crossing of this gene onto a susceptible mouse background, and this is now in progress in our laboratory.

ACKNOWLEDGMENTS

We thank Sue Priola, Kim Hasenkrug, and Sonja Best for critical reviews of the manuscript; Anita Mora and Gary Hettrick for technical assistance with graphics; and Cynthia Favara for technical assistance with histology.

REFERENCES

1. **Banisadr, G., F. Queraud-Lesaux, M. C. Boutterin, D. Pelaprat, B. Zalc, W. Rostene, F. Haour, and S. M. Parsadaniantz.** 2002. Distribution, cellular localization and functional role of CCR2 chemokine receptors in adult rat brain. J. Neurochem. **81:**257–269.
2. **Bell, J. E.** 1998. The neuropathology of adult HIV infection. Rev. Neurol. **154:**816–829.
3. **Baruch, A. B., L. Xu, P. R. Young, K. Bengali, J. J. Oppenheim, and J. M. Wang.** 1995. Monocyte chemotactic protein-3 (MCP3) interacts with multiple leukocyte receptors. C-C CKR1, a receptor for macrophage inflammatory protein-1 alpha/Rantes, is also a functional receptor for MCP3. J. Biol. Chem. **270:**22123–22128.
4. **Carbone, K. M., S. A. Rubin, Y. Nishino, and M. V. Pletnikov.** 2001. Borna disease: virus-induced neurobehavioral disease pathogenesis. Curr. Opin. Microbiol. **4:**467–475.
5. **Chen, B. P., W. A. Kuziel, and T. E. Lane.** 2001. Lack of CCR2 results in increased mortality and impaired leukocyte activation and trafficking following infection of the central nervous system with a neurotropic coronavirus. J. Immunol. **167:**4585–4592.
6. **Conant, K., A. Garzino-Demo, A. Nath, J. C. McArthur, W. Halliday, C. Power, R. C. Gallo, and E. O. Major.** 1998. Induction of monocyte chemoattractant protein-1 in HIV-1 Tat-stimulated astrocytes and elevation in AIDS dementia. Proc. Natl. Acad. Sci. USA **95:**3117–3121.
7. **Eugenin, E. A., T. G. D'Aversa, L. Lopez, T. M. Calderon, and J. W. Berman.** 2003. MCP-1 (CCL2) protects human neurons and astrocytes from NMDA or HIV-tat-induced apoptosis. J. Neurochem. **85:**1299–1311.

8. **Fuentes, M. E., S. K. Durham, M. R. Swerdel, A. C. Lewin, D. S. Barton, J. R. Megill, R. Bravo, and S. A. Lira.** 1995. Controlled recruitment of monocytes and macrophages to specific organs through transgenic expression of monocyte chemoattractant protein-1. J. Immunol. **155:**5769–5776.
9. **Galasso, J. M., M. J. Miller, R. M. Cowell, J. K. Harrison, J. S. Warren, and F. S. Silverstein.** 2000. Acute excitotoxic injury induces expression of monocyte chemoattractant protein-1 and its receptor, CCR2, in neonatal rat brain. Exp. Neurol. **165:**295–305.
10. **Glabinski, A. R., V. Balasingam, M. Tani, S. L. Kunkel, R. M. Strieter, V. W. Yong, and R. M. Ransohoff.** 1996. Chemokine monocyte chemoattractant protein-1 is expressed by astrocytes after mechanical injury to the brain. J. Immunol. **156:**4363–4368.
11. **Gong, X., W. Gong, D. B. Kuhns, A. Ben Baruch, O. M. Howard, and J. M. Wang.** 1997. Monocyte chemotactic protein-2 (MCP-2) uses CCR1 and CCR2B as its functional receptors. J. Biol. Chem. **272:**11682–11685.
12. **Gonzalez, E., B. H. Rovin, L. Sen, G. Cooke, R. Dhanda, S. Mummidi, H. Kulkarni, M. J. Bamshad, V. Telles, S. A. Anderson, E. A. Walter, K. T. Stephan, M. Deucher, A. Mangano, R. Bologna, S. S. Ahuja, M. J. Dolan, and S. K. Ahuja.** 2002. HIV-1 infection and AIDS dementia are influenced by a mutant MCP-1 allele linked to increased monocyte infiltration of tissues and MCP-1 levels. Proc. Natl. Acad. Sci. USA **99:**13795–13800.
13. **He, J., Y. Chen, M. Farzan, H. Choe, A. Ohagen, S. Gartner, J. Busciglio, X. Yang, W. Hofmann, W. Newman, C. R. Mackay, J. Sodroski, and D. Gabuzda.** 2000. CCR3 and CCR5 are co-receptors for HIV-1 infection of microglia. Nature **385:**645–649.
14. **Huffnagle, G. B., L. K. McNeil, R. A. McDonald, J. W. Murphy, G. B. Toews, N. Maeda, and W. A. Kuziel.** 1999. Cutting edge: role of C-C chemokine receptor 5 in organ-specific and innate immunity to *Cryptococcus neoformans*. J. Immunol. **163:**4642–4646.
15. **Kaul, M., and S. A. Lipton.** 1999. Chemokines and activated macrophages in HIV gp120- induced neuronal apoptosis. Proc. Natl. Acad. Sci. USA **96:** 8212–8216.
16. **Kelder, W., J. C. McArthur, T. Nance-Sproson, D. McClernon, and D. E. Griffin.** 1998. Beta-chemokines MCP-1 and RANTES are selectively increased in cerebrospinal fluid of patients with human immunodeficiency virus-associated dementia. Ann. Neurol. **44:**831–835.
17. **Kolson, D. L., E. Lavi, and F. Gonzalez-Scarano.** 1998. The effects of human immunodeficiency virus in the central nervous system. Adv. Virus Res. **50:** 1–47.
18. **Kurihara, T., G. Warr, J. Loy, and R. Bravo.** 1997. Defects in macrophage recruitment and host defense in mice lacking the CCR2 chemokine receptor. J. Exp. Med. **186:**1757–1762.
19. **Kuziel, W. A., T. C. Dawson, M. Quinones, E. Garavito, G. Chenaux, S. S. Ahuja, R. L. Reddick, and N. Maeda.** 2003. CCR5 deficiency is not protective in the early stages of atherogenesis in *apoE* knockout mice. Atherosclerosis **167:**25–32.
20. **Kuziel, W. A., S. J. Morgan, T. C. Dawson, S. Griffin, O. Smithies, K. Ley, and N. Maeda.** 1997. Severe reduction in leukocyte adhesion and monocyte extravasation in mice deficient in CC chemokine receptor 2. Proc. Natl. Acad. Sci. USA **94:**12053–12058.
21. **Lynch, W. P., A. H. Sharpe, and E. Y. Snyder.** 1999. Neural stem cells as engraftable packaging lines can mediate gene delivery to microglia: evidence from studying retroviral env-related neurodegeneration. J. Virol. **73:**6841–6851.
22. **McGeer, P. L., and E. G. McGeer.** 2002. Local neuroinflammation and the progression of Alzheimer's disease. J. Neurovirol. **8:**529–538.
23. **Mennicken, F., R. Maki, E. B. de Souza, and R. Quirion.** 1999. Chemokines and chemokine receptors in the CNS: a possible role in neuroinflammation and patterning. Trends Pharmacol. Sci. **20:**73–78.
24. **Peters, W., H. M. Scott, H. F. Chambers, J. L. Flynn, I. F. Charo, and J. D. Ernst.** 2001. Chemokine receptor 2 serves an early and essential role in resistance to *Mycobacterium tuberculosis*. Proc. Natl. Acad. Sci. USA **98:** 7958–7963.
25. **Peterson, K. E., S. J. Robertson, J. L. Portis, and B. Chesebro.** 2001. Differences in cytokine and chemokine responses during neurological disease induced by polytropic murine retroviruses map to separate regions of the viral envelope gene. J. Virol. **75:**2848–2856.
26. **Portis, J. L., S. Czub, S. Robertson, F. McAtee, and B. Chesebro.** 1995. Characterization of a neurologic disease induced by a polytropic murine retrovirus: evidence for differential targeting of ecotropic and polytropic viruses in the brain. J. Virol. **69:**8070–8075.
27. **Poulsen, D. J., C. Favara, E. Y. Snyder, J. Portis, and B. Chesebro.** 1999. Increased neurovirulence of polytropic mouse retroviruses delivered by inoculation of brain with infected neural stem cells. Virology **263:**23–29.
28. **Robertson, M. N., M. Miyazawa, S. Mori, B. Caughey, L. H. Evans, S. F. Hayes, and B. Chesebro.** 1991. Production of monoclonal antibodies reactive with a denatured form of the Friend murine leukemia virus gp70 envelope protein: use in a focal infectivity assay, immunohistochemical studies, electron microscopy and western blotting. J. Virol. Methods **34:**255–271.
29. **Robertson, S. J., K. J. Hasenkrug, B. Chesebro, and J. L. Portis.** 1997. Neurologic disease induced by polytropic murine retroviruses: neurovirulence determined by efficiency of spread to microglial cells. J. Virol. **71:**5287–5294.
30. **Sarafi, M. N., E. A. Garcia-Zepeda, J. A. MacLean, I. F. Charo, and A. D. Luster.** 1997. Murine monocyte chemoattractant protein (MCP)-5: a novel CC chemokine that is a structural and functional homologue of human MCP-1. J. Exp. Med. **185:**99–109.
31. **Sarzotti, M.** 1997. Immunologic tolerance. Curr. Opin. Hematol. **4:**48–52.
32. **Sauder, C., and J. C. de la Torre.** 1999. Cytokine expression in the rat central nervous system following perinatal Borna disease virus infection. J. Neuroimmunol. **96:**29–45.
33. **Schmidtmayerova, H., H. S. Nottet, G. Nuovo, T. Raabe, C. R. Flanagan, L. Dubrovsky, H. E. Gendelman, A. Cerami, M. Bukrinsky, and B. Sherry.** 1996. Human immunodeficiency virus type 1 infection alters chemokine beta peptide expression in human monocytes: implications for recruitment of leukocytes into brain and lymph nodes. Proc. Natl. Acad. Sci. USA **93:**700–704.
34. **Snyder, E. Y., D. L. Deitcher, C. Walsh, S. Arnold-Aldea, E. A. Hartwieg, and C. L. Cepko.** 1992. Multipotent neural cell lines can engraft and participate in development of mouse cerebellum. Cell **68:**33–51.
35. **Traister, R. S., and W. P. Lynch.** 2002. Reexamination of amphotropic murine leukemia virus neurovirulence: neural stem cell-mediated microglial infection fails to induce acute neurodegeneration. Virology **293:**262–272.
36. **Trgovcich, J., J. F. Aronson, J. C. Eldridge, and R. E. Johnston.** 1999. TNFalpha, interferon, and stress response induction as a function of age-related susceptibility to fatal Sindbis virus infection of mice. Virology **263:** 339–348.
37. **Vago, L., M. Nebuloni, S. Bonetto, A. Pellegrinelli, P. Zerbi, A. Ferri, E. Lavri, M. Capra, M. P. Grassi, and G. Costanzi.** 2001. Rantes distribution and cellular localization in the brain of HIV-infected patients. Clin. Neuropathol. **20:**139–145.
38. **Wells, T. N., C. A. Power, and A. E. Proudfoot.** 1998. Definition, function and pathophysiological significance of chemokine receptors. Trends Pharmacol. Sci. **19:**376–380.
39. **Wesselingh, S. L., C. Power, J. D. Glass, W. R. Tyor, J. C. McArthur, J. M. Farber, J. W. Griffin, and D. E. Griffin.** 1993. Intracerebral cytokine messenger RNA expression in acquired immunodeficiency syndrome dementia. Ann. Neurol. **33:**576–582.
40. **Xia, M. Q., and B. T. Hyman.** 1999. Chemokines/chemokine receptors in the central nervous system and Alzheimer's disease. J. Neurovirol. **5:**32–41.
41. **Zink, M. C., G. D. Coleman, J. L. Mankowski, R. J. Adams, P. M. Tarwater, K. Fox, and J. E. Clements.** 2001. Increased macrophage chemoattractant protein-1 in cerebrospinal fluid precedes and predicts simian immunodeficiency virus encephalitis. J. Infect. Dis. **184:** 1015–1021.